ACCOUNTS of chemical research

Article

pubs.acs.org/accounts

Synthetic Heme/Copper Assemblies: Toward an Understanding of Cytochrome *c* Oxidase Interactions with Dioxygen and Nitrogen Oxides

Published as part of the Accounts of Chemical Research special issue "Synthesis in Biological Inorganic Chemistry".

Shabnam Hematian, Isaac Garcia-Bosch,[§] and Kenneth D. Karlin*

Department of Chemistry, Johns Hopkins University, Baltimore, Maryland 21211, United States

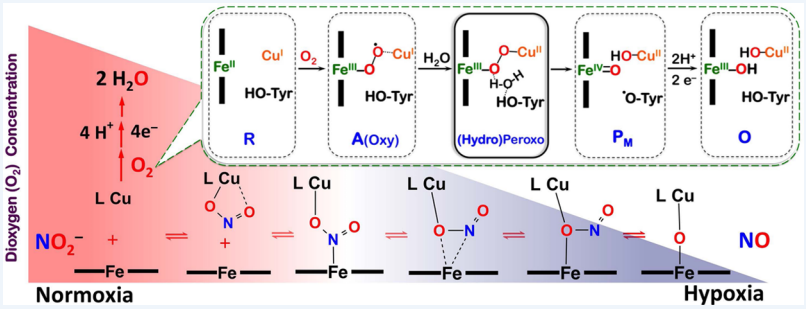

CONSPECTUS: Our long-time niche in synthetic biological inorganic chemistry has been to design ligands and generate coordination complexes of copper or iron ions or both, those reacting with dioxygen (O_2) or nitrogen oxides (e.g., nitric oxide ($NO_{(g)}$) and nitrite (NO_2^-)) or both. As inspiration for this work, we turn to mitochondrial cytochrome *c* oxidase, which is responsible for dioxygen consumption and is also the predominant target for $NO_{(g)}$ and nitrite within mitochondria. In this Account, we highlight recent advances in studying synthetic heme/Cu complexes in two respects. First, there is the design, synthesis, and characterization of new O_2 adducts whose further study will add insights into O_2 reductive cleavage chemistry. Second, we describe how related heme/Cu constructs reduce nitrite ion to $NO_{(g)}$ or the reverse, oxidize $NO_{(g)}$ to nitrite. The reactions of nitrogen oxides occur as part of C*c*O's function, which is intimately tied to cellular O_2 balance.

We had first discovered that reduced heme/Cu compounds react with O_2 giving μ-oxo heme-Fe^{III}–O–Cu^{II}(L) products; their properties are discussed. The *O*-atom is derived from dioxygen, and interrogations of these systems led to the construction and characterization of three distinctive classes of heme–peroxo complexes, two high-spin and one low-spin species.

Recent investigations include a new approach to the synthesis of low-spin heme–peroxo–Cu complexes, employing a "naked" synthon, where the copper ligand denticity and geometric types can be varied. The result is a collection of such complexes; spectroscopic and structural features (by DFT calculations) are described. Some of these compounds are reactive toward reductants/protons effecting subsequent O–O cleavage. This points to how subtle improvements in ligand environment lead to a desired local structure and resulting optimized reactivity, as known to occur at enzyme active sites.

The other sector of research is focused on heme/Cu assemblies mediating the redox interplay between nitrite and $NO_{(g)}$. In the nitrite reductase chemistry, the cupric center serves as a Lewis acid, while the heme is the redox active center providing the electron. The orientation of nitrite in approaching the ferrous heme center and *N*-atom binding are important. Also, detailed spectroscopic and kinetic studies of the $NO_{(g)}$ oxidase chemistry, in excellent agreement with theoretical calculations, reveal the intermediates and key mechanistic steps. Thus, we suggest that both chemical and biochemical heme/Cu-mediated nitrite reductase and $NO_{(g)}$ oxidase chemistry require *N*-atom binding to a ferrous heme along with cupric ion *O*-atom coordination, proceeding via a three-membered O–Fe–N chelate ring transition state. These important mechanistic features of heme/Cu systems interconverting $NO_{(g)}$ and nitrite are discussed for the first time.

1. INTRODUCTION

Mitochondrial cytochrome *c* oxidase (C*c*O) is the terminal component of the respiratory chain that carries out the enzymatic four-electron reduction of dioxygen (O_2) to water (H_2O). This enzyme is essential to respiration, providing the energy to produce a proton gradient across the membrane, which supplies the driving force for ATP synthesis. The binding of O_2 and its subsequent reduction to water take place at the C*c*O binuclear active site consisting of heme-a_3 and Cu_B ligated by three histidine residues with a unique linkage of one histidine to a nearby tyrosine residue. During catalytic turnover, the Fe^{II}/Cu^{I} center binds and reduces O_2, sequentially forming superoxide (**A**), (hydro)peroxide, and ferryl ($\mathbf{P_M}$, after O–O cleavage, thought

Received: May 23, 2015
Published: August 5, 2015

DOI: 10.1021/acs.accounts.5b00265
Acc. Chem. Res. 2015, 48, 2462–2474

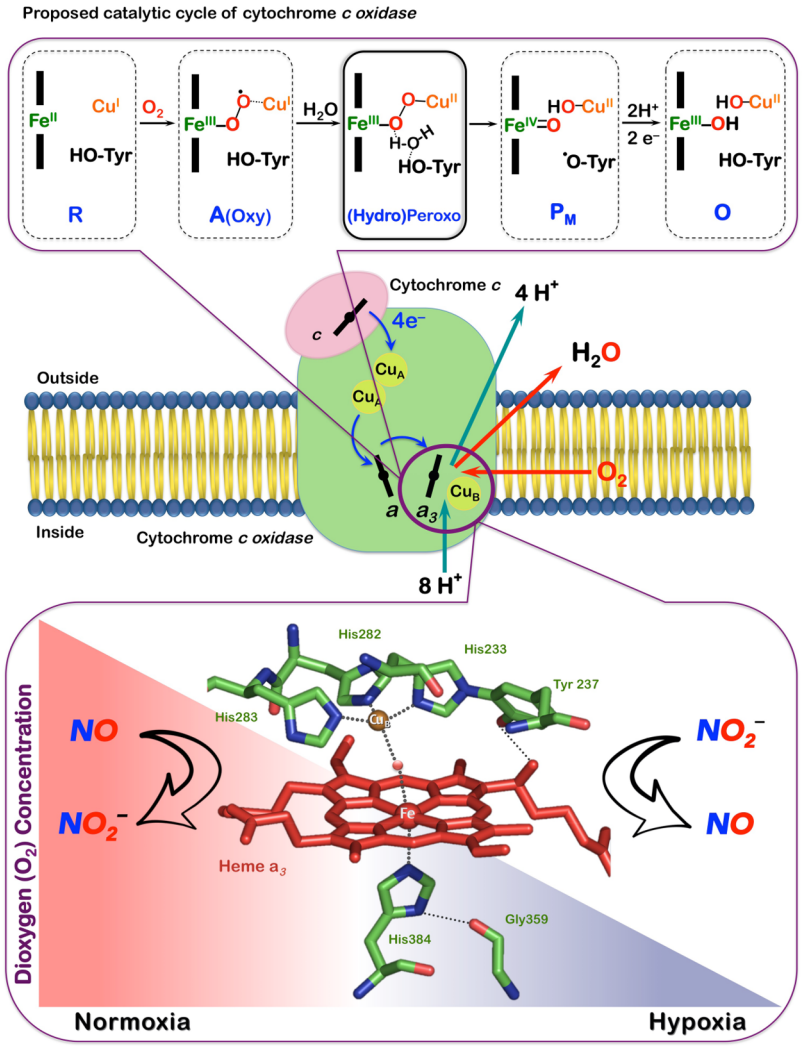

Figure 1. Cytochrome *c* oxidase reduces dioxygen via the proposed intermediates shown (top). This heme-a_3/Cu_B binuclear active site also functions in NO_2^-/$NO_{(g)}$ interconversion in a regulatory role modulating O_2 balance (bottom).

to be assisted by tyrosine H atom injection) intermediates (Figure 1), followed by stepwise protonation−reduction giving water and regenerating the Fe^{II}/Cu^{I} site.[1−3] The O−O bond reductive cleavage event is a crucial but complicated process; it depends on electron transfer and protonation steps, and its full understanding has implications well beyond C*c*O.[4]

This same heme-a_3/Cu_B binuclear center is also a major site of respiratory regulation as it interacts with nitrite (NO_2^-) and nitric oxide ($NO_{(g)}$) to modulate cellular O_2 balance (Figure 1). In tissues experiencing hypoxia, when the O_2 concentration decreases below physiological levels,[5] nitrite serves as an acceptor for accumulating electrons at the C*c*O binuclear active site, and the enzymatic one-electron reduction of nitrite (NO_2^-) takes place generating nitric oxide. The $NO_{(g)}$ produced by C*c*O reversibly interacts with the same center and, thus, decreases its affinity to O_2 reduction resulting in cellular O_2 accumulation. Some of mitochondrially produced $NO_{(g)}$ also participates in the up-regulation of hypoxic nuclear genes (hypoxic signaling).[5,6] In turn, at mitochondrial sites recovering from hypoxia, local accumulation of O_2 progressively triggers one-electron oxidation of $NO_{(g)}$ back to NO_2^- ion, the latter held in reserve to be reconverted when needed. This process serves as an adaptive mechanism eliminating $NO_{(g)}$-mediated respiratory inhibition.[7,8]

In this Account, we describe our recent findings on both subjects. A great emphasis has been placed on design and generation of relevant O_2 adducts, that is, heme-Fe−(O_2^{2-})−Cu(L) complexes, as a segue to future chemistries involving the critical O−O cleavage process. We also highlight our investigations on the interconversion of $NO_{(g)}$ and nitrite mediated by heme/Cu assemblies. Our work is thus aimed at introducing synthetic heme/Cu binuclear systems capable of performing chemical transformations of relevant small molecules, those occurring at the C*c*O active site. Our goal is to provide fundamental insights into essential factors contributing to these redox processes.

2. INITIAL WORK ON HEME-Fe^{II}···Cu^{I}(L)/O_2 CHEMISTRY: Fe^{III}−OXO−Cu^{II} COMPLEXES

Our initial attempts at modeling the C*c*O heme-a_3/Cu_B dioxygen chemistry led to discovery of μ-oxo heme-Fe^{III}−O−Cu^{II}(L) compounds forming from reaction of O_2 with equimolar quantities of the corresponding reduced heme and copper mononuclear complexes; the μ-oxo ligand derives from O_2. Interestingly, despite the known substantial thermodynamic stability of μ-oxo iron dimer heme-Fe^{III}−O−Fe^{III}-heme, here such μ-oxo heme-Fe^{III}−O−Cu^{II}(L) complexes are the kinetically stable

DOI: 10.1021/acs.accounts.5b00265
Acc. Chem. Res. 2015, 48, 2462−2474

Chart 1. Molecular Structures of μ-Oxo [(Porphyrinate)Fe^{III}–O–Cu^{II}(L)]$^+$ Complexes[a]

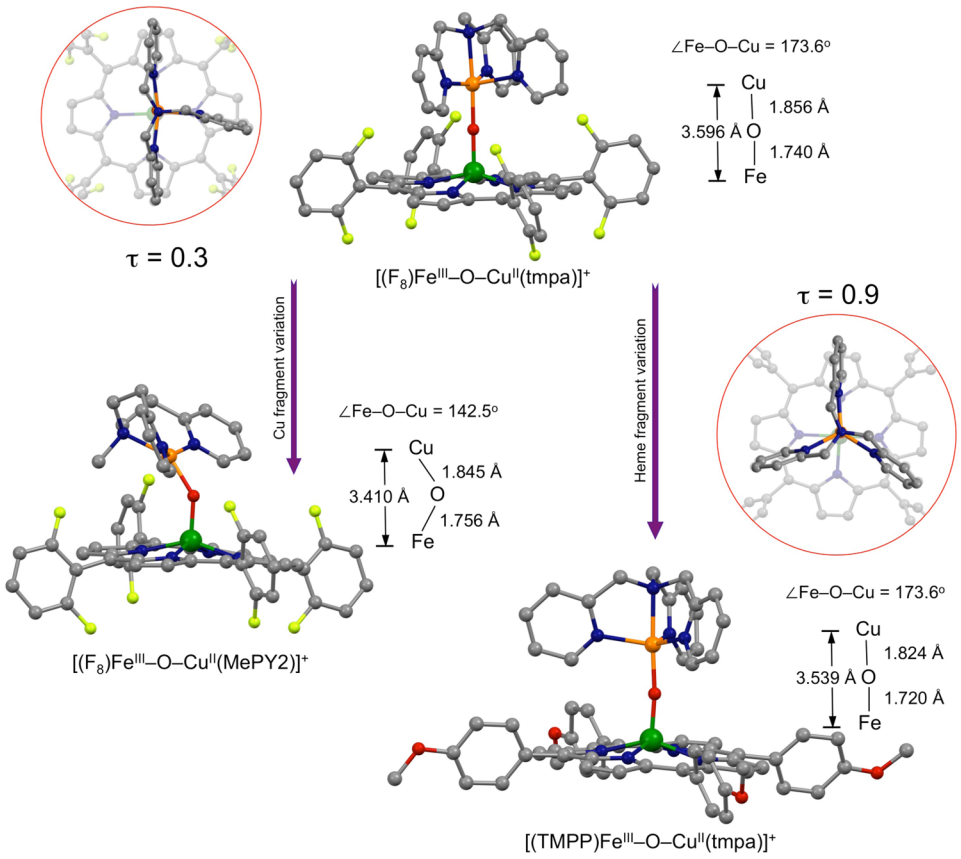

[a]Abbreviations: tmpa, tris(2-pyridylmethylamine); MePY2, bis(2-pyridyl-ethyl)methylamine; F_8, tetrakis(2,6-difluorophenyl)-porphyrinate(2−); TMPP, tetrakis(4-methoxyphenyl)porphyrinate(2−).

products, which can also be generated by acid–base reaction of oxidized metal complexes, that is, reaction of heme-Fe^{III}–OH and [(L)Cu^{II}] plus a base.[9,10]

We recently added new crystal structures, [(TMPP)Fe^{III}–O–Cu^{II}(tmpa)]$^+$ and [(F$_8$)Fe^{III}–O–Cu^{II}(MePY2)]$^+$ (Chart 1), to our library of such compounds, which conform to previous findings in that the Fe–O–Cu core in the former compound with its tetradentate chelate for the cupric center, TMPA, is near-linear while the latter complex bearing a tridentate copper(II) ligand, MePY2, has a very bent μ-oxo moiety (Chart 1). They also exhibit the very red-shifted Soret bands (λ_{max} = 443 and 438 nm, respectively) characteristic of the μ-oxo compounds relative to that of classical high-spin ferric hemes, probably due to a weaker affinity of Cu(II) for the bridging oxo and thus the greater degree of π charge donation available onto the ferric center by the oxo group. Also, [(TMPP)Fe^{III}–O–Cu^{II}(tmpa)]$^+$ is the first example of the heme-Fe^{III}–O–Cu^{II}(L) class that contains the strongly donating TMPP porphyrinate. Notably, comparison of [(TMPP)Fe^{III}–O–Cu^{II}(tmpa)]$^+$ and its closely related analog [(F$_8$)Fe^{III}–O–Cu^{II}(tmpa)]$^+$, in which only the porphyrinate identity varies, reveals that the cupric centers adopt very different geometries; for the former, the tmpa-Cu N$_4$O ligation occurs within a nearly perfect trigonal bipyramidal (TBP) geometry (τ = 0.9), while for the latter, the copper center adjusts to a distorted square pyramidal (SP) coordination (τ = 0.3, Chart 1). Steric constraints imposed by *o*-fluorine substituents of the *meso*-phenyl groups on the attached porphyrin ring in the F$_8$ ligand dictate structural properties of the cupric center resulting in deviation from the normal TBP geometry seen for [(tmpa)Cu^{II}(X)]$^{n+}$ (X = H$_2$O, MeCN, Cl$^-$, or NO$_2^-$) compounds.[11]

In all μ-oxo compounds, the bridging oxo moiety is very basic and can be reversibly protonated to give the protonated acid–base partner, heme-Fe^{III}–(OH)–Cu^{II}(L). For some cases corresponding μ-hydroxo analogues have been characterized and pK_a values reported.[12,13] In general, protonation of the Fe–O–Cu core results in bending and rehybridization of the bridging oxygen moiety, accompanied by bond elongation.

3. HIGH-SPIN HEME–PEROXO–COPPER COMPLEXES

In view of our interest in studying the CcO active-site O$_2$-reduction chemistry (Figure 1), Fe/Cu/O$_2$ intermediates preceding the formation of μ-oxo heme-Fe^{III}–O–Cu^{II}(L) compounds have been primary targets for study. A first generation example is the metastable heme–peroxo–copper complex [(F$_8$)Fe^{III}–(O$_2^{2-}$)–Cu^{II}(tmpa)]$^+$ (**HS-TMPA**, Scheme 1), formed from O$_2$ bubbling through cold solutions of a 1:1 mixture of [(tmpa)Cu^{I}(MeCN)]$^+$/(F$_8$)Fe^{II}.[14] Structural and spectroscopic studies on **HS-TMPA** provided evidence for a bridging peroxide unit bound in a side-on fashion to the high-spin iron(III) center and end-on to the copper(II) center.[15] Key observations were as follows: (i) ^{2}H-NMR spectroscopy revealed that **HS-TMPA** possesses antiferromagnetically coupled (through the peroxide bridge) high-spin iron(III) and copper(II) ions, leading to an S = 2 system; (ii) resonance Raman spectroscopic (rRaman) measurements identified O–O, Fe–O, and Cu–O vibrations (Scheme 1); (iii) X-ray absorption fine structure (EXAFS) provided Cu–O, Fe–O, and

DOI: 10.1021/acs.accounts.5b00265
Acc. Chem. Res. 2015, 48, 2462–2474

Scheme 1

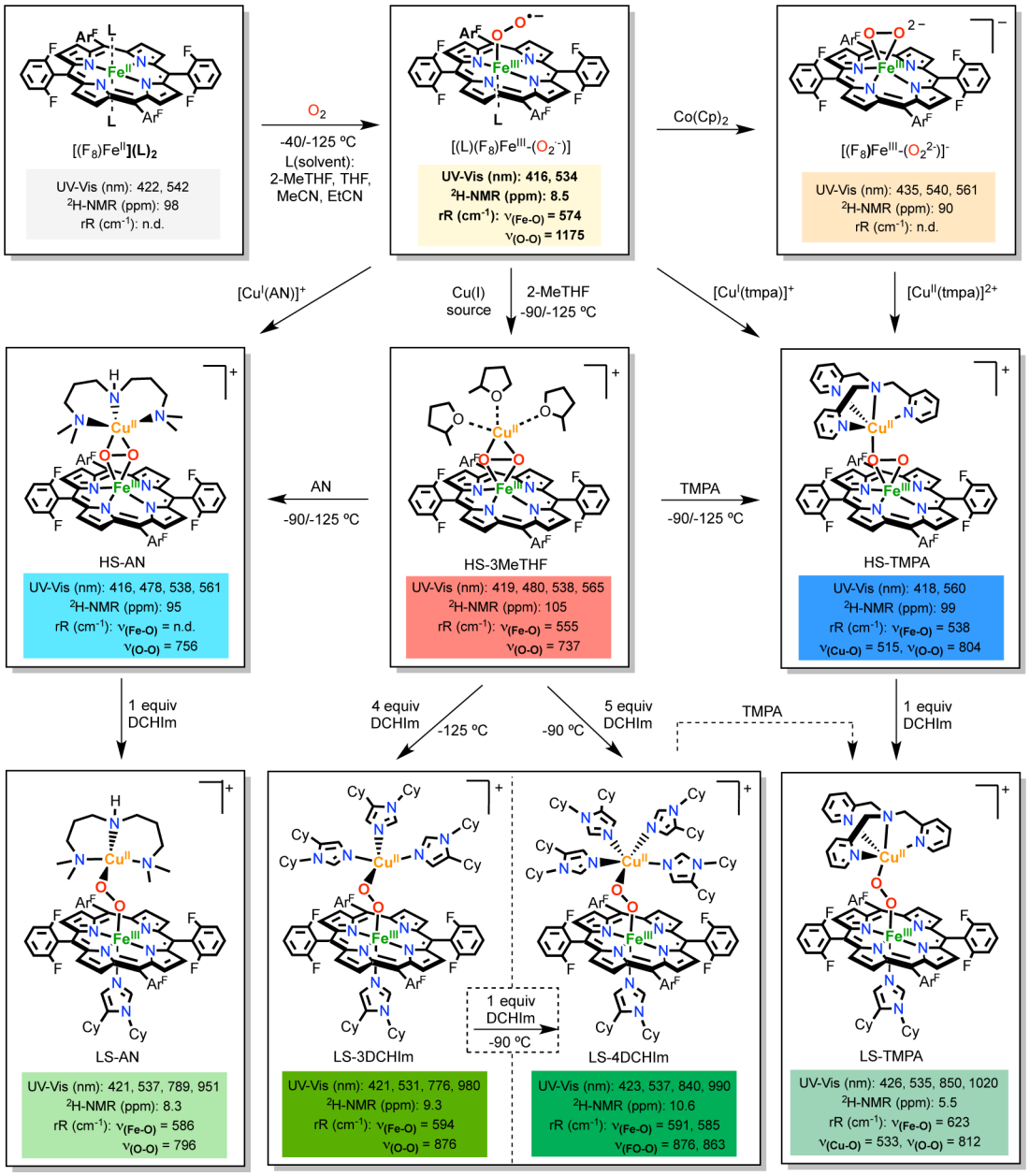

Fe···Cu contributions at 1.87, 1.94, and 3.72 Å. These spectroscopic/structural features correspond to data from the only crystallographically characterized heme−peroxo−copper system.[16]

As to the formation of **HS-TMPA**, stopped-flow UV−vis measurements revealed an iron(III)−superoxo intermediate $[(L)(F_8)Fe^{III}-(O_2^{\bullet-})]$ (L = solvent, that is, EtCN) initially formed. Indeed, addition of 1 equiv of $[(tmpa)Cu^{I}(MeCN)]^+$ to this leads to **HS-TMPA**. Scheme 1 depicts alternative synthetic routes giving **HS-TMPA**. With the expectation that significant (or even small) ligand variations can dramatically alter structure and other properties, we also synthesized heme−(O_2)−copper assemblies using tridentate chelates for copper. A well-studied example is $[(F_8)Fe^{III}-(O_2^{2-})-Cu^{II}(AN)]^+$ (**HS-AN**, AN is 3,3′-iminobis(*N*,*N*-dimethylpropylamine), Scheme 1; EXAFS, Fe···Cu = 3.63 Å). Further analyses led to the conclusion that **HS-AN** and other analogs with tridentate ligands for copper possess a side-on peroxide coordination mode (i.e., μ-η^2:η^2) to both metal ions (Scheme 1).[17,18]

4. LOW-SPIN HEME−PEROXO−COPPER COMPLEX, LS-AN

A crucial advance for our research came when we reported the generation of the low-spin (LS) $[(DCHIm)(F_8)Fe^{III}-(O_2^{2-})-Cu^{II}(AN)]^+$ (**LS-AN**),[19] likely a close analogue of the putative heme−peroxo−copper species formed in CcO. Addition of an axial ligand (DCHIm = 1,5-dicyclohexylimidazole) to **HS-AN** leads to the new species **LS-AN**, which presented unusually strong low-energy UV−vis features (Scheme 1). A change in the spin-state is associated with an alternation in the bridging mode of the peroxide ligand, forming an end-on $Fe^{III}-(\mu$-η^1:η^1-$O_2^{2-})-Cu^{II}$ core. ^{2}H-NMR spectroscopy indicates an overall $S = 0$ spin-state, derived from antiferromagnetic coupling of a low-spin Fe(III) ($S = 1/2$) to the $S = 1/2$ Cu(II). Two isotope-sensitive

DOI: 10.1021/acs.accounts.5b00265
Acc. Chem. Res. 2015, 48, 2462−2474

features at 796 and 586 cm^{-1} are assigned to O−O and Fe−O vibrations, respectively, based on rRaman. Note the large change in ν_{O-O} in comparing high- and low-spin AN analogs. EXAFS measurements on **LS-AN** give Cu−O, Fe−O, and Fe···Cu distances of 1.98, 1.81, and 4.01 Å, respectively. Relative to **HS-AN**, a shortening of the Fe−O bond (1.94 vs 1.81 Å) and elongation of the Fe···Cu distance (3.72 vs 4.01 Å) provide for the new end-on peroxide bridging mode in **LS-AN** (Scheme 1).

5. "NAKED" Fe−PEROXO−Cu SYNTHON FOR NEW LOW-SPIN COMPOUNDS

We recently explored a new synthetic approach,[20] following a discovery leading to the high-spin complex $[(F_8)Fe^{III}-(O_2^{2-})-Cu^{II}(MeTHF)_3]^+$ (**HS-3MeTHF**, Scheme 1), a "naked" synthon as a starting point for the generation of an array of heme−peroxo−copper assemblies. Addition of $[Cu^{I}(CH_3CN)_4][B(C_6F_5)_4]$ to a solution of $[(MeTHF)(F_8)Fe^{III}-(O_2^{\bullet-})]$ at low temperatures (−90 to −125 °C) leads to the clean formation of **HS-3MeTHF**, formulated as possessing a side-on $Fe^{III}-(\mu\text{-}\eta^2\text{:}\eta^2\text{-}O_2^{2-})-Cu^{II}$ core with three solvent molecules surrounding the copper(II) center, due to its spectroscopic similarities with **HS-AN**, see Scheme 1 for spectroscopic data.

The utility of **HS-3MeTHF** is illustrated by its use in generation of a new low-spin complex $[(DCHIm)(F_8)Fe^{III}-(O_2^{2-})-Cu^{II}(tmpa)]^+$ (**LS-TMPA**, Scheme 1). Addition of 1 equiv of the free ligand TMPA to the **HS-3MeTHF** gives **HS-TMPA** by replacement of the labile solvent ligands to copper. A further step comes from addition of 1 equiv of DCHIm to **HS-TMPA**, giving the new compound **LS-TMPA**. Like **LS-AN**, **LS-TMPA** also possesses unusual low-energy UV−vis features (Scheme 1). ^{2}H-NMR spectroscopy confirmed the change in spin-state, as the pyrrole signal shifted from 99 ppm for **HS-TMPA** ($S = 2$) to 5 ppm for **LS-TMPA** ($S = 0$). The change in the spin state is again linked to alteration in the peroxide coordination mode. The data given in Scheme 1 shows that O−O, Fe−O, and Cu−O stretching frequencies for **LS-TMPA** are systematically higher than those for **HS-TMPA**, especially the ν_{Fe-O} value. This appears to be the first case in which the effect of changing the spin state on all relevant vibrations, O−O, Fe−O, and Cu−O, could be evaluated.[20]

Most interestingly, we found that simple monodentate ligand donors such as imidazoles, native C*c*O active-site ligands, could be added to the solvato "naked" complex **HS-3MeTHF** to generate new low-spin heme−(O_2)−copper assemblies. Addition of excess of DCHIm to **HS-3MeTHF** at −125 °C led to the formation of a new species with UV−vis features very similar to those found for **LS-AN**. Titration experiments provided evidence that 4 equiv of DCHIm were required for its formation, formulating the new low-spin peroxo as $[(DCHIm)(F_8)Fe^{III}-(O_2^{2-})-Cu^{II}(DCHIm)_3]^+$ (**LS-3DCHIm**) with one imidazole ligand coordinated to the heme and three coordinated to the cupric ion. ^{2}H-NMR spectroscopic characterization corroborated the $S = 0$ complex ground state, while rRaman revealed the existence of a particularly high O−O stretching vibration, ν_{O-O} = 876 cm^{-1} (Scheme 1).[20]

When **LS-3DCHIm** is warmed to −90 °C in the presence of excess DCHIm, a new species with shifted UV−vis features forms (Scheme 1). The same species is also obtained when 5 equiv of DCHIm are added to **HS-3MeTHF** generated at −90 °C. Cooling this new complex with four imidazole donors for the copper ion, $[(DCHIm)(F_8)Fe^{III}-(O_2^{2-})-Cu^{II}(DCHIm)_4]^+$ (**LS-4DCHIm**, Scheme 1) does not lead to the reversible formation of **LS-3DCHIm**; thus, **LS-4DCHIm** is the thermodynamic product, formed after the generation of the kinetic product, **LS-3DCHIm**. ^{2}H-NMR spectroscopy indicates that these two complexes are distinctly different (Scheme 1). However, **LS-4DCHIm** has distinctive but surprisingly similar vibrational features to those found for **LS-3DCHIm**, ν_{Fe-O} = 594 cm^{-1} and ν_{O-O} = 876 cm^{-1}; coordination of an extra imidazole does not induce dramatic changes in the Fe−O and O−O bond strengths. Interestingly, the compounds **LS-3DCHIm** and **LS-4DCHIm** can also be used as starting material for the generation of other low-spin compounds. In fact, addition of 1 equiv of TMPA to **LS-3DCHIm** or **LS-4DCHIm** results in imidazole ligand displacement, giving **LS-TMPA**.[20]

6. STRUCTURAL VARIATIONS AND COMPARISON OF HEME−PEROXO−COPPER CORES

As described above, we have synthesized a series of heme−peroxo−Cu(L) complexes with varying ligands (L) to Cu(II) ion and observed that spectroscopic parameters for L = TMPA vs AN vs (3 or 4) DCHIm exhibit distinctive differences. Thus, there are clear differences in structure and bonding (electronic structure) among the compounds. With Ed Solomon's group at Stanford University, DFT calculations have been carried out in order to determine finer details concerning structural and vibrational characteristics of these compounds.[20] One focus was to compare and contrast the (**HS-AN**)/(**LS-AN**) pair. We see that axial base coordination (DCHIm) promotes isomerization of the side-on $Fe^{III}-(\mu\text{-}\eta^2\text{:}\eta^2\text{-}O_2^{2-})-Cu^{II}$ core in **HS-AN**, giving an end-on $Fe^{III}-(\mu\text{-}\eta^1\text{:}\eta^1\text{-}O_2^{2-})-Cu^{II}$ structure in **LS-AN**, responsible for the change in spin-state. A significant reorganization of the peroxo core has occurred, as evidenced by the increased Fe···Cu distance (+0.36 Å) and shortened Fe−O (−0.20 Å), O−O (−0.06 Å), and Cu−O (−0.09 Å) bond lengths (Figure 2). These changes stem from (i) the transition to an end-on geometry in which the Fe and Cu ions bind only one oxygen atom and (ii) the low-spin nature of heme-iron(III). The O−O distance shortening is small but can be explained by an increase in O_2^{2-} (π^*) donation into the Fe(d_{z^2}) orbital, which increases the O−O bond strength. Similarly, DFT calculations on the (**HS-TMPA**)/(**LS-TMPA**) pair lead to similar observed trends (Figure 2).[20] DCHIm coordination as a heme axial ligand produces rearrangement of the peroxo core with a notorious increase in the Fe−Cu distance (+0.77 Å) but shortened Fe−O (−0.20 Å) and O−O (−0.06 Å) distances (Figure 2, bottom right). However, in this case, only a slight change in the geometry around copper center is observed (Cu−O distance shortened 0.02 Å), which is explained by the retention of the peroxide coordination mode (i.e., end-on to Cu) upon heme-Fe spin change.

We have previously mentioned[21] that heme−peroxo−copper reactivity is enhanced in the low-spin-state. Thus, comparison of **LS-AN** and **LS-TMPA** is worthy of discussion. They both possess end-on $Fe^{III}-(\mu\text{-}\eta^1\text{:}\eta^1\text{-}O_2^{2-})-Cu^{II}$ low-spin cores; however, their structural differences (Figure 2) are prominent. A significantly greater Fe···Cu distance (+0.50 Å) and much larger ∠Cu−O−O (+22°) are found for **LS-TMPA**. As shown before, these variances are also reflected in the complexes' distinctive spectroscopic features (UV−vis, rRaman). Ongoing computational studies will include analyses of **LS-3DCHIm** vs **LS-4DCHIm** and comparison to the other low-spin complexes. These complexes possess the same ν_{O-O} values (876 cm^{-1}; vide supra), but this frequency is much higher (>64 cm^{-1}) than what is found for **LS-AN** or **LS-TMPA**.[20]

DOI: 10.1021/acs.accounts.5b00265
Acc. Chem. Res. 2015, 48, 2462−2474

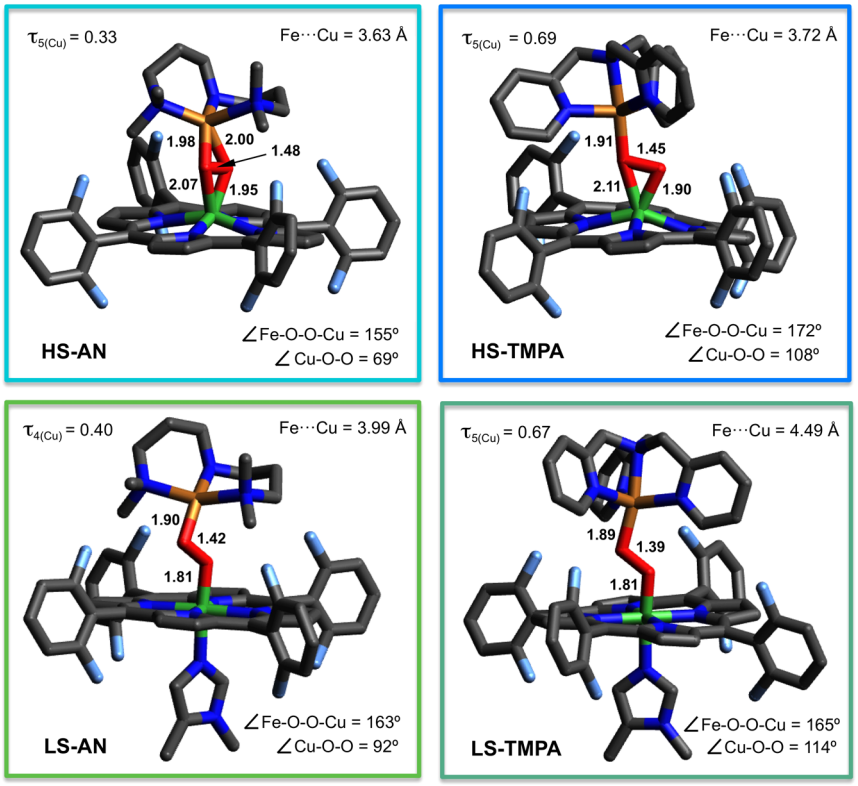

Figure 2. DFT optimized structures for **HS-AN**, **LS-AN**, **HS-TMPA**, and **LS-TMPA** complexes. Adapted with permission from ref 20. Copyright 2015 American Chemical Society.

As seen from the structural and spectroscopic information displayed in Scheme 1 and Figure 2, significant variations are observed as a function of the nature of the specific ligand to copper ion and the heme spin state. Peroxo-bridged heme/Cu species are possible C*c*O reaction intermediates forming between **Oxy** and $\mathbf{P_M}$ (Figure 1);[19,20,22,23] we regard them as a near ideal starting point for studying O−O reductive cleavage reactivity.[24] Further, initial studies reveal that **LS-3DCHIm** and **LS-4DCHIm**, along with other compounds (Scheme 1), possess markedly different behavior with respect to O−O cleavage upon protonation or reduction. Our long-term goal is to understand these reactivity differences in terms of heme−peroxo−Cu complex structure and bonding variations, and the results will impact C*c*O chemistry and other processes where O−O reductive cleavage occurs (see Introduction).

7. INITIAL WORK ON NITRITE AND $NO_{(g)}$ INTERCONVERSION

In biological systems, the production of $NO_{(g)}$ as a signaling agent, for example, in smooth muscle cell relaxation, is critically important. Aside from $NO_{(g)}$ synthesis by cytochrome P-450 like NO-synthases, which produce $NO_{(g)}$ via L-arginine oxidative chemistry,[25] nitrite also serves as a critical $NO_{(g)}$ source (also see below). The cellular balance of $NO_{(g)}$ is very tightly regulated and mechanisms for its removal include $NO_{(g)}$-reductase (NOR), coupling $NO_{(g)}$ molecules to give N_2O, and $NO_{(g)}$-dioxygenase (NOD), producing nitrate as a benign $NO_{(g)}$ oxidation product.[25] $NO_{(g)}$ is also "removed" via oxidation to nitrite, to later be converted back to nitric oxide when needed. The blood copper protein ceruloplasmin oxidizes $NO_{(g)}$ to nitrite,[26] as does cytochrome *c* oxidase.

In fact, our heme/Cu assemblies as heme-a_3/Cu_B C*c*O active-site models not only are capable of O_2 reduction but also possess redox activity toward nitrogen oxides including nitrite and $NO_{(g)}$ interconversions. To help shed light on the molecular mechanism of this redox interplay between these two molecules and the roles that the metal centers may play, we have employed our binuclear synthetic systems. In our initial report,[27] we introduced a synthetic heme/Cu assembly that in its partially reduced form facilitates nitrite reduction to $NO_{(g)}$. Thus, addition of the cupric−nitrite complex $[(tmpa)Cu^{II}(NO_2)]^+$ to 2 equiv of the ferrous heme $(F_8)Fe^{II}$ (λ_{max} = 421 nm) resulted in formation of a one-to-one mixture of the ferrous heme−nitrosyl complex $(F_8)Fe^{II}(NO)$ (λ_{max} = 399 nm) and the μ-oxo compound $[(F_8)Fe^{III}-O-Cu^{II}(tmpa)]^+$ (λ_{max} = 435 nm, Scheme 2), readily confirmed by UV−vis, EPR, and IR (ν_{NO} = 1688 cm^{-1}) spectroscopies. Here, the second equivalent of ferrous heme was not involved in the redox chemistry and only trapped the $NO_{(g)}$ produced. Our electrochemical measurements showed that in this heme/Cu assembly, the cuprous complex $[(tmpa)Cu^{I}(MeCN)]^+$ (−0.42 V vs $Fc^{+/0}$) is a chemically stronger reductant compared with the ferrous heme $(F_8)Fe^{II}$ (−0.20 V vs $Fc^{+/0}$). However, based on our control experiments, neither of these reduced compounds, nor the combination of the two, is capable of reducing nitrite to $NO_{(g)}$. Thus, our initial study[27] highlighted two primary findings: (i) the ferrous heme is the redox active center providing the electron, (ii) while the cupric center serves as a Lewis acid facilitating nitrite (N−O) bond cleavage. This overall chemical transformation can also be viewed as one-electron reduction of nitrite (formally NO^+), which accompanies a transfer of an oxygen atom derived from the nitrite, finally forming an oxo-bridge $Fe^{III}-O-Cu^{II}$ product.

Interestingly, in turn, we showed that the fully oxidized form of the same assembly as a μ-oxo compound $[(F_8)Fe^{III}-O-Cu^{II}(tmpa)]^+$ (λ_{max} = 435 nm) could oxidize $NO_{(g)}$ back to nitrite (Scheme 2).[27] Addition of $NO_{(g)}$ to the μ-oxo complex

DOI: 10.1021/acs.accounts.5b00265
Acc. Chem. Res. 2015, 48, 2462−2474

Scheme 2. Heme/Cu-Assembly-Mediated Interconversion of Nitrite and Nitric Oxide

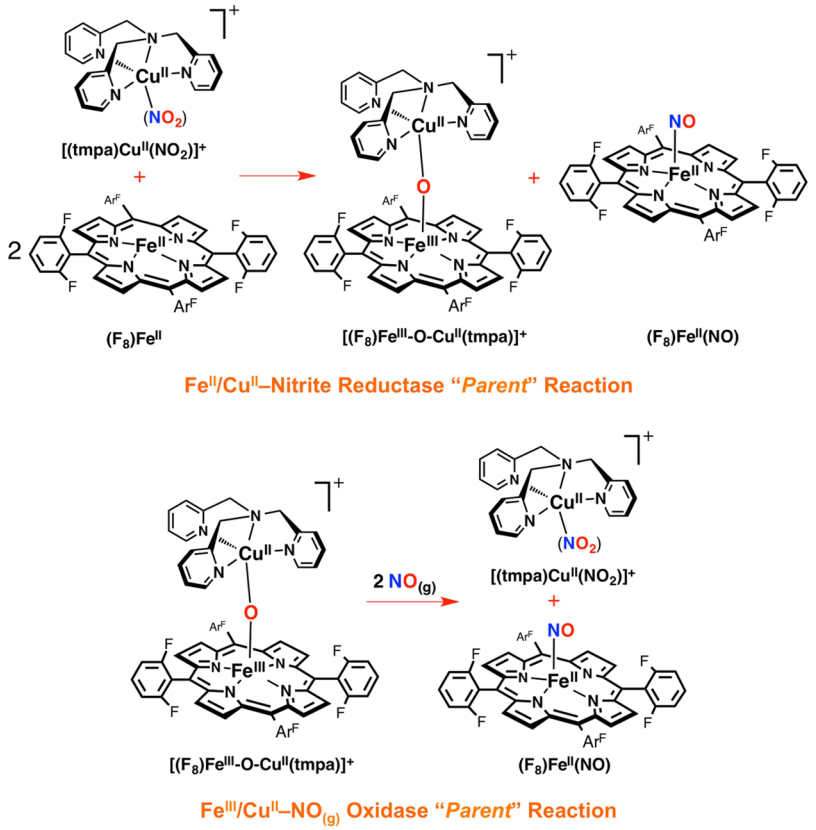

$[(F_8)Fe^{III}-O-Cu^{II}(tmpa)]^+$ resulted in reformation of the cupric–nitrite complex $[(tmpa)Cu^{II}(NO_2)]^+$; the reduced heme $(F_8)Fe^{II}$ formed from this $NO_{(g)}$ oxidase chemistry is trapped by a second equivalent of $NO_{(g)}$ to give $(F_8)Fe^{II}(NO)$ (λ_{max} = 399 nm). The results of product analysis using UV–vis, EPR, and IR spectroscopies and capillary electrophoresis (nitrite analysis, 95% yield) confirmed the nature of the products and proposed stoichiometric reaction. For comparison, the μ-hydroxo complex $[(F_8)Fe^{III}-(OH)-Cu^{II}(tmpa)]^{2+}$ was also tested for "$NO_{(g)}$ oxidase" chemistry, but addition of $NO_{(g)}$ resulted in no nitrite production; the μ-oxo complex $[(F_8)Fe^{III}-O-Cu^{II}(tmpa)]^+$ is unique in its ability to effect this redox and oxo transfer reaction.

8. INVESTIGATION ON NITRITE REDUCTASE CHEMISTRY MEDIATED BY HEME/Cu ASSEMBLIES

To further investigate the key factors involved in the nitrite reductase chemistry, the nature of the heme or the copper ligand or both were synthetically modified (Scheme 3).[28]

8.1. Pophyrinate Variation

Toward a better understanding of the role of the reducing ability of the ferrous heme center, a different tetraarylporphyrinate bearing strong electron-donating peripheral groups, TMPP, was employed, and its reactivity was compared with the Fe^{II}/Cu^{II}–nitrite "parent" reaction, the combination of $[(tmpa)Cu^{II}(NO_2)]^+$ and $(F_8)Fe^{II}$, where the heme possesses electron-withdrawing peripheral substituents.[28] Product analysis confirmed the same overall redox reaction, converting nitrite to $NO_{(g)}$, thus generating a one-to-one mixture of the μ-oxo compound $[(TMPP)Fe^{III}-O-Cu^{II}(tmpa)]^+$ (λ_{max} = 443 nm) and ferrous heme nitrosyl complex $(TMPP)Fe^{II}(NO)$ (λ_{max} = 410 nm).

Scheme 3. Nitrite Reductase Chemistry Mediated by Heme/Cu Assemblies[a]

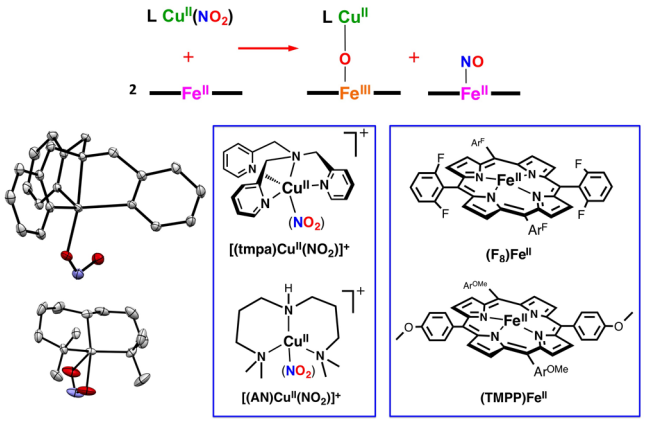

[a](top) General reaction equation. (bottom) Structures of copper and heme complexes used in our study.

Notably, on the basis of UV–vis monitoring of the disappearance of the Soret band for the ferrous heme, the reaction proceeds at about the same rate as for the Fe^{II}/Cu^{II}–nitrite "parent" reaction, pointing to the fact that even with the greater electron-donating ability of the ferrous heme $(TMPP)Fe^{II}$, the nitrite reduction reaction is not accelerated.

8.2. Influence of Copper Coordination Environment on Nitrite Reduction

In order to examine the effect of differing modes of coordination of nitrite to the cupric center, we employed $[(AN)Cu^{II}(NO_2)](CF_3SO_3)$, having a tridentate alkylamine chelate rather than

DOI: 10.1021/acs.accounts.5b00265
Acc. Chem. Res. 2015, 48, 2462–2474

a tetradentate pyridyl-alkylamine ligand, as in $[(tmpa)Cu^{II}(NO_2)][B(C_6F_5)_4]$ (Scheme 3).[28] As revealed by X-ray crystallography, these two cupric−nitrite complexes exhibit different binding modes of nitrite to the copper center, *O,O′*-bidentate binding in the former and *O*-unidentate coordination in the latter (note that the outer *O*-atom is very accessible). Reactions of both cupric−nitrite complexes with either ferrous-heme leads to the same overall redox reaction reducing nitrite to $NO_{(g)}$. Interestingly, we observed that when $[(AN)Cu^{II}(NO_2)]^+$ was reacted with either $(F_8)Fe^{II}$ or $(TMPP)Fe^{II}$, the rate of ferrous heme disappearance was roughly twice as fast as the reaction of the same heme with the $[(tmpa)Cu^{II}(NO_2)]^+$. Thus, faster reduction of nitrite to $NO_{(g)}$ occurs when the nitrito ligand is coordinated in bidentate vs unidentate fashion to the cupric center. We concluded that this difference in nitrite coordination mode leads to differing approaches of the cupric−nitrite compound to the reduced heme (i.e., the reduction center) to transiently form a bridged ferrous heme−(nitrite)−cupric complex. For $[(AN)Cu^{II}(NO_2)]^+$, having *O,O′*-bidentate nitrite ligation, one could anticipate a facile approach of a nitrite nitrogen atom to the ferrous heme, leading to a nitro (*N*-ligated) mode of coordination (Figure 3), perhaps in the rate-determining step.

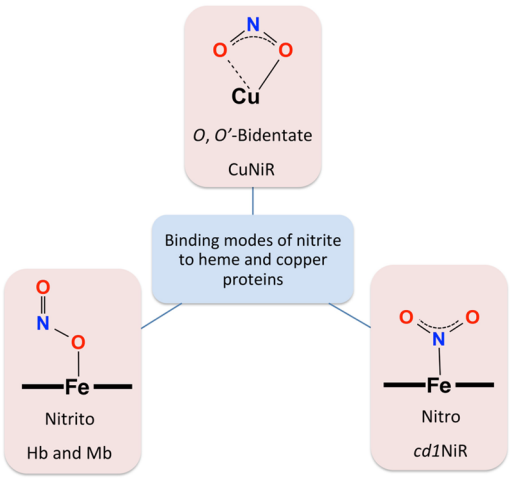

Figure 3. Binding modes of nitrite to heme and copper proteins.

This can be followed by an intramolecular electron transfer from the ferrous heme to the bridging nitrite generating a bridged hydronitrite radical (NO_2^{2-}) assembly, which rapidly converts to $NO_{(g)}$ and a kinetically stable μ-oxo (O^{2-}) complex $[(porphyrinate)Fe^{III}-O-Cu^{II}(AN)]^+$ (F_8 or TMPP porphyrinate).[28]

Another possibility is that in both cases, using $[(tmpa)Cu^{II}(NO_2)]^+$ or $[(AN)Cu^{II}(NO_2)]^+$, NO_2^- binding to the ferrous heme must occur through the nitrogen atom in order to lead to a productive reaction, that is, resulting in nitrite (N−O) bond cleavage and $NO_{(g)}$ formation. This would be consistent with the expectation that soft Fe(II) favors the softer *N*-atom coordination versus that hard *O*-atom of nitrite based on "hard−soft" acid−base principles. So, even for $[(tmpa)Cu^{II}(NO_2)]^+$, an effective reaction may require a relatively slow nitrite group rearrangement or reorientation in order that the nitrogen atom can bind the ferrous heme. Such a rearrangement is not required for the nitrite bound in $[(AN)Cu^{II}(NO_2)]^+$; thus a faster reaction occurs, all consistent with the observations.

In general, enzymatic nitrite reductase reactivity (i.e., one-electron reduction of nitrite to $NO_{(g)}$) has been ascribed to two classes of proteins, containing either copper (CuNiR) or heme (e.g., cd_1NiR, hemoglobin (Hb), and myoglobin (Mb)) as cofactor.[25,29,30] As Figure 3 illustrates, based on available crystal structure data, nitrite binds to copper-containing NiRs in the *O,O′*-bidentate nitrito mode, while it coordinates to cd_1NiR via the *N*-unidentate nitro fashion. It has also been shown that nitrite binding to Hb or Mb occurs through an *O*-unidentate coordination (nitrito mode).[31,32] Interestingly, the interactions of nitrite with ba_3-*Cc*O, with both heme and copper active-site ions, have been just recently studied by rRaman,[32] revealing the existence of a ferrous heme−nitro species not previously observed. This finding, thus, supports our original hypothesis or thought[28] that iron−nitrogen bond formation, as assisted by cupric center orienting or directing of the nitrite ion, is a crucial step in our heme/Cu assembly nitrite-reductase activity. Further support for this supposition is also provided through our detailed mechanistic study of the reverse reaction, that is, oxidation of $NO_{(g)}$ to nitrite, discussed below.

9. MECHANISTIC STUDY OF NITRIC OXIDE OXIDASE CHEMISTRY MEDIATED BY HEME/Cu ASSEMBLIES

As indicated in Scheme 3, we initially[27] described in the $Fe^{III}/Cu^{II}-NO_{(g)}$ "parent" reaction a fully oxidized heme/Cu assembly, in the form of the μ-oxo complex $[(F_8)Fe^{III}-O-Cu^{II}(tmpa)]^+$, which mediates the one-electron oxidation of $NO_{(g)}$ to nitrite. To expand on the initial study, we very recently reported a detailed mechanistic study[11] using different μ-oxo $[(porphyrinate)Fe^{III}-O-Cu^{II}(L)]^+$ complexes in which the heme or copper chelating ligand is modified (Scheme 4); ligand (L) for the cupric core was either a tripodal tetradentate pyridyl-alkylamine chelate or a related tridentate alkylamine ligand, and two different tetraarylporphyrinates were employed for the heme core, one with electron-withdrawing peripheral substituents versus one with strong electron-donating groups.

9.1. Copper Coordination Environment Variation

The effects of alterations in copper-ligand denticity and electronics were investigated by comparing the tetradentate chelate TMPA used in the $Fe^{III}/Cu^{II}-NO_{(g)}$ oxidase "parent" reaction with new tridentate ligands, L = AN and MePY2 (Scheme 4).[11] When the tridentate chelates were employed under the same experimental conditions, oxidation of $NO_{(g)}$ by μ-oxo $[(F_8)Fe^{III}-O-Cu^{II}(L)]^+$ ensued considerably faster than that for the parent analog, still yielding the Cu(II)−nitrite plus ferrous heme−nitrosyl products.

These observations can be justified based on two factors: (i) previous studies reveal that for μ-oxo heme-$Fe^{III}-O-Cu^{II}(L)$ complexes where L is the tridentate ligand AN or MePY2,[13] the bridging oxo ion is more basic than that for the tetradentate ligand, that is, L = TMPA,[12] and (ii) for tridentate ligands, there is a lack of steric hindrance, primarily because the $Fe^{III}-O-Cu^{II}$ moiety is bent; further, the coordination number for the copper ion is only four, relative to pentacoordination in the TMPA analog, making the bridging oxo ion more accessible for addition of $NO_{(g)}$ (Chart 1 and Scheme 4).[11]

9.2. Impact of Peripheral Substituents of the Porphyrinate: Dynamics and Intermediates Involved in $NO_{(g)}$ Oxidase by Heme/Cu Assemblies

Modification of the nature of the porphyrinate employed in this chemistry has turned out to provide us with many new mechanistic insights.[11] A new μ-oxo complex, $[(TMPP)Fe^{III}-O-Cu^{II}(tmpa)]^+$, was synthesized and characterized, and in its reaction with $NO_{(g)}$ at RT, there was an instantaneous change

DOI: 10.1021/acs.accounts.5b00265
Acc. Chem. Res. 2015, 48, 2462−2474

Scheme 4. Variations of Heme/Cu Assemblies in $NO_{(g)}$ Oxidase Chemistry

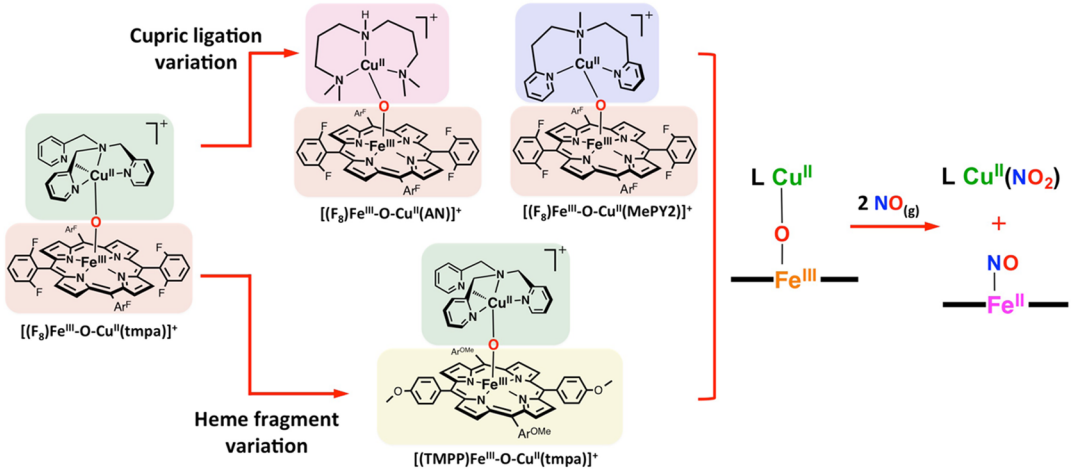

Scheme 5. Proposed Reaction Steps for $NO_{(g)}$ Oxidase Chemistry Mediated by μ-Oxo Heme-Fe^{III}–O–Cu^{II}(L) Complexes Generating Nitrite

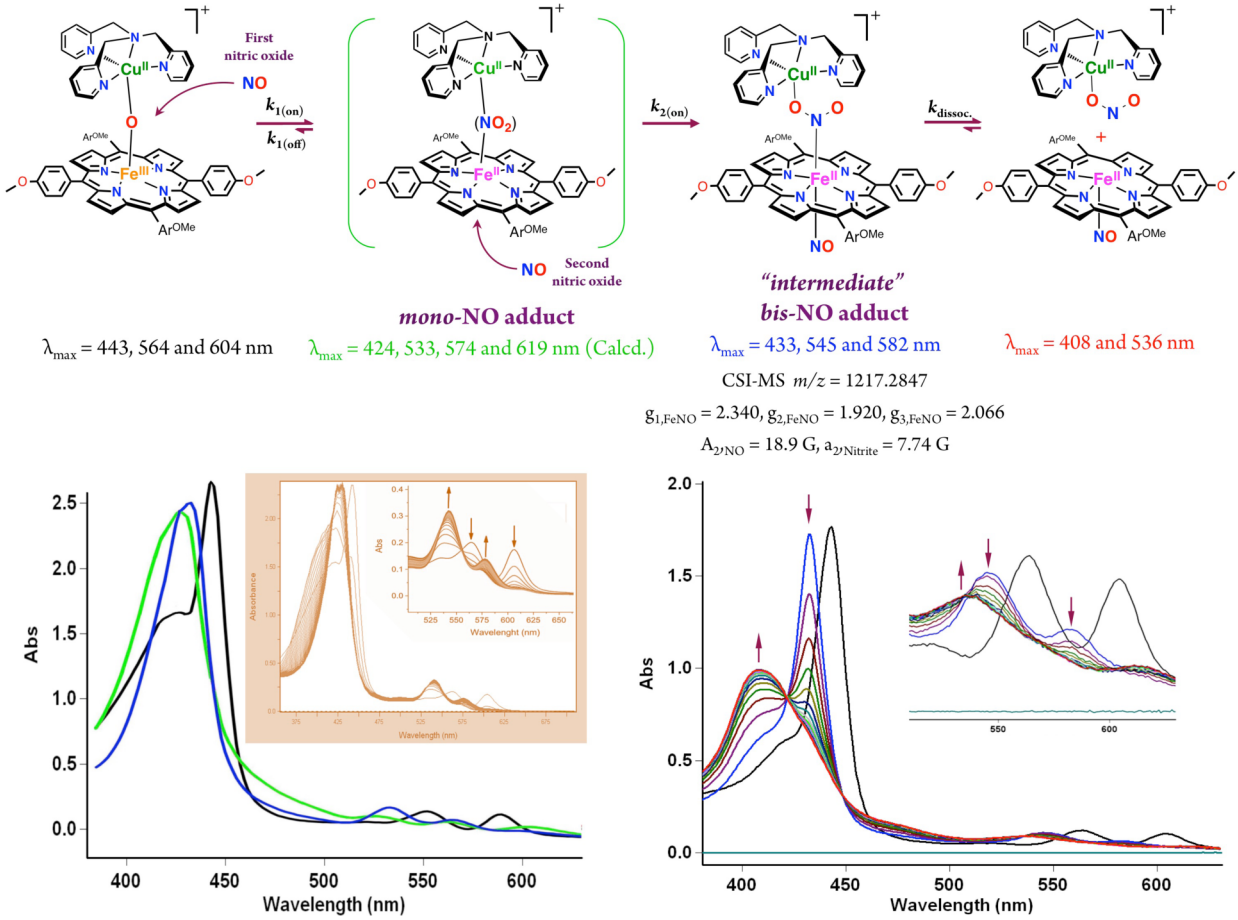

Adapted with permission from ref 11. Copyright 2015 American Chemical Society

(as followed by UV–vis monitoring), giving a mixture of species, which eventually all converted to the expected final products, $[(tmpa)Cu^{II}(NO_2)]^+$ and $(TMPP)Fe^{II}(NO)$.

When this reaction was repeated at −20 °C, a new intermediate (λ_{max} = 433 nm) was detected following addition of $NO_{(g)}$ to the solution of μ-oxo compound.[11] Later, this isosbestically converted to the final products in a first-order process (Scheme 5, $k_{dissoc} = 6.7 \times 10^{-3}$ s^{-1} at −20 °C, $\Delta H^{\ddagger} = 41.1 \pm 0.1$ kJ mol^{-1} and $\Delta S^{\ddagger} = -123 \pm 2$ J mol^{-1} K^{-1}). In cryospray ionization mass spectrometry (CSI-MS) measurements[33] at −60 °C, we could detect this new species, which presented itself as a manifold of intense peaks with maximum at m/z = 1217.2847, this corresponding to a bis-NO adduct of the initial μ-oxo compound. With this observation, along with the further studies carried

DOI: 10.1021/acs.accounts.5b00265
Acc. Chem. Res. 2015, 48, 2462–2474

out (vide infra), we could conclude that sequential addition of two $NO_{(g)}$ molecules to the starting $[(TMPP)Fe^{III}–O–Cu^{II}(tmpa)]^+$ complex led to the bis-NO adduct, formulated as $[(NO)(TMPP)Fe^{II}–NO_2–Cu^{II}(tmpa)]^+$ complex.[11]

Low-temperature stopped-flow kinetic spectroscopic measurements[33] provided (full) spectral changes for the entire course of the reaction. From the analyses carried out, the spectrum of the mono-NO adduct, which forms prior to formation of the bis-NO intermediate, could be extracted (Scheme 5). We also determined corresponding observed rate constants for the addition of first ($k_{1(obs)}$) and the second ($k_{2(obs)}$) $NO_{(g)}$ molecules for a range of low temperatures down to −83 °C and different $NO_{(g)}$ concentrations (ranging between 0.28 to 2.3 mM).[11] At all temperatures, linear dependencies ($k_{(obs)} = k_{(on)}[NO] + k_{(off)}$) of the observed rate constants ($k_{1(obs)}$ and $k_{2(obs)}$) on $NO_{(g)}$ concentration were observed. An overview of the first and second $NO_{(g)}$ binding kinetics at different temperatures and thermodynamic parameters are given in Table 1. Notably, the binding of the second $NO_{(g)}$ is irreversible; addition of the first $NO_{(g)}$ to $[(TMPP)Fe^{III}–O–Cu^{II}(tmpa)]^+$ occurs about 1 order of magnitude faster than binding of the second $NO_{(g)}$ (Scheme 5, Table 1).[11,34]

Table 1. Binding Kinetics and Thermodynamics of First and Second $NO_{(g)}$ to $[(TMPP)Fe^{III}–O–Cu^{II}(tmpa)]^+$

	first $NO_{(g)}$ binding		*second* $NO_{(g)}$ binding
T (°C)	$k_{1(on)}$ (M^{-1} s^{-1})	$k_{1(off)}$ (s^{-1})	$k_{2(on)}$ (M^{-1} s^{-1})
−60	6053 ± 186	2.61 ± 0.24	706 ± 20
−67	5061 ± 244	1.47 ± 0.32	637 ± 40
−74	2356 ± 69	1.07 ± 0.09	504 ± 40
−83	1184 ± 12	0.50 ± 0.01	*a*

first $NO_{(g)}$ binding				*second* $NO_{(g)}$ binding	
$\Delta H^{\ddagger}_{(on)}$ (kJ mol^{-1})	$\Delta S^{\ddagger}_{(on)}$ (J mol^{-1} K^{-1})	$\Delta H^{\ddagger}_{(off)}$ (kJ mol^{-1})	$\Delta S^{\ddagger}_{(off)}$ (J mol^{-1} K^{-1})	$\Delta H^{\ddagger}_{(on)}$ (kJ mol^{-1})	$\Delta S^{\ddagger}_{(on)}$ (J mol^{-1} K^{-1})
24 ± 3	−64 ± 10	22 ± 2	−131 ± 9	7 ± 2	−155 ± 8

first $NO_{(g)}$ binding	
$\Delta H°$ (kJ mol^{-1})	$\Delta S°$ (J mol^{-1} K^{-1})
2.0 ± 0.4	67 ± 15

[a]Could not be determined.[11]

The small values of $\Delta H^{\ddagger}_{(on)}$ and negative activation entropies ($\Delta S^{\ddagger}_{(on)}$) observed are consistent with the associative nature of the $NO_{(g)}$ binding steps. The negligible activation enthalpy (7 ± 2 kJ mol^{-1}) for the binding of the second $NO_{(g)}$ points to an almost activation-less process. Together with the negative $\Delta S^{\ddagger}_{(on)}$ value, one can conclude that the rate-determining step does not involve bond breaking; instead, bond-making predominates. These data and conclusions are in excellent agreement with DFT studies[33] (Scheme 6), which also describe the sequential addition of $NO_{(g)}$ to the μ-oxo complex.[11]

The first $NO_{(g)}$ attacks the μ-oxo atom, leading to the mono-NO adduct (Scheme 6). According to DFT calculations, electron-transfer occurs here, formally from $NO_{(g)}$ to the heme, via transient formation of a "triangular" structure. Both the original μ-oxo atom and the $NO_{(g)}$-derived *N*-atom bind to the iron center (Scheme 6, TS1). The experimentally observed low activation enthalpy (24 ± 3 kJ/mol) and negative activation entropy derived from the kinetic studies are consistent with this sequence of events.[11]

As relevant to the addition of the second $NO_{(g)}$ molecule, the DFT results reveal that the SOMO of the bis-NO "intermediate" is predominantly localized on the Fe-porphyrin moiety, pointing to its ferrous character. Experimental evidence confirming the formulation and properties of the "intermediate" were obtained from (i) the fact that cooling the products, consisting of a 1:1 mixture of $(TMPP)Fe^{II}(NO)$ plus $[(tmpa)Cu^{II}(NO_2)]^+$, leads to association and reformation of the key 433 nm UV–vis feature of the "intermediate", where the nitrite bound to copper ion coordinates and thus forms a bridge to the ferrous heme–nitrosyl complex; (ii) analyses of EPR spectra of the "intermediate" indicate the presence of a six-coordinated ferrous-heme nitrosyl bearing a trans *N*-based ligand ($a_{2,Nitrite}$ = 7.74 G), all linked to an EPR active cupric species in a TBP coordination environment.[11]

In the last step, the "intermediate", undergoes dissociation in a first-order process to release the finally observed mononuclear adducts, the cupric–nitrite and ferrous heme–nitrosyl complexes.

10. BROADER PERSPECTIVES ON NITRITE AND $NO_{(g)}$ INTERCONVERSION

From our broad investigations on nitrite/$NO_{(g)}$ redox interconversions mediated by heme/Cu centers, we conclude that both (bio)chemical transformations necessitate specific nitrite coordination, *N*-atom to ferrous-heme and *O*-atom to cupric ion. In fact, we believe that both chemical transformations proceed via the same intermediates.

Our proposed mechanism for nitrite reduction is represented by the forward (left-to-right) reaction in Scheme 7. For aerobic organisms, O_2 is the ultimate electron acceptor for cellular respiration. Under conditions of stress and when the O_2 concentration drops below a certain level, nitrite starts to compete with the residual O_2 for reduction by the C*c*O binuclear active site, eventually generating $NO_{(g)}$. The $NO_{(g)}$ thus produced reversibly inhibits the oxygen reduction at the same center and allows for O_2 accumulation. Then, in this recovery from hypoxia, the reverse reaction consists of the same steps traversed backward; $NO_{(g)}$ is removed and converted back to nitrite for future use. Now, in normoxia, in the absence of $NO_{(g)}$, the C*c*O recovers its traditional function, that is, catalyzing the four-electron reduction of O_2 to water.

We note that the μ-oxo heme-Fe^{III}–O–Cu^{II}(L) complexes described here may not exactly represent C*c*O turnover intermediates or even resting-state structures. However, these μ-oxo compounds should be thought of as representatives of actual enzyme active site heme/Cu entities, those involved in $NO_{(g)}$ oxidation chemistry, possibly a heme-Fe^{III}–OH···Cu^{II} or even a high-valent compound II type species, heme-Fe^{IV}=O···Cu.

11. SUMMARY AND OUTLOOK

In this Account, we have described our recent studies using synthetic heme/Cu assemblies, investigating their reactivity with dioxygen and nitrogen oxides. The work involves rational design and implementation of constructs mimicking basic aspects of the C*c*O active site, which allow for redox transformations of these small molecules (i.e., O_2, $NO_{(g)}$, and NO_2^-).

Our long time goals have been to study metal–dioxygen chemistry at heme/Cu centers, because the details of O_2 ligation, resulting coordination geometry, and electronic structure require full elucidation. Because clean four-electron, four-proton O_2 reduction will depend on heme and Cu ligation, factors such as the exact juxtaposition of these two metal ions, redox potentials ($Fe^{III/II}$, $Fe^{IV/III}$, and $Cu^{II/I}$), relative basicity of O_2-derived

DOI: 10.1021/acs.accounts.5b00265
Acc. Chem. Res. 2015, 48, 2462–2474

Scheme 6. Schematic Calculated Energy Profile for $[(TMPP)Fe^{III}–O–Cu^{II}(tmpa)]^+$ Reaction with $NO_{(g)}$[a]

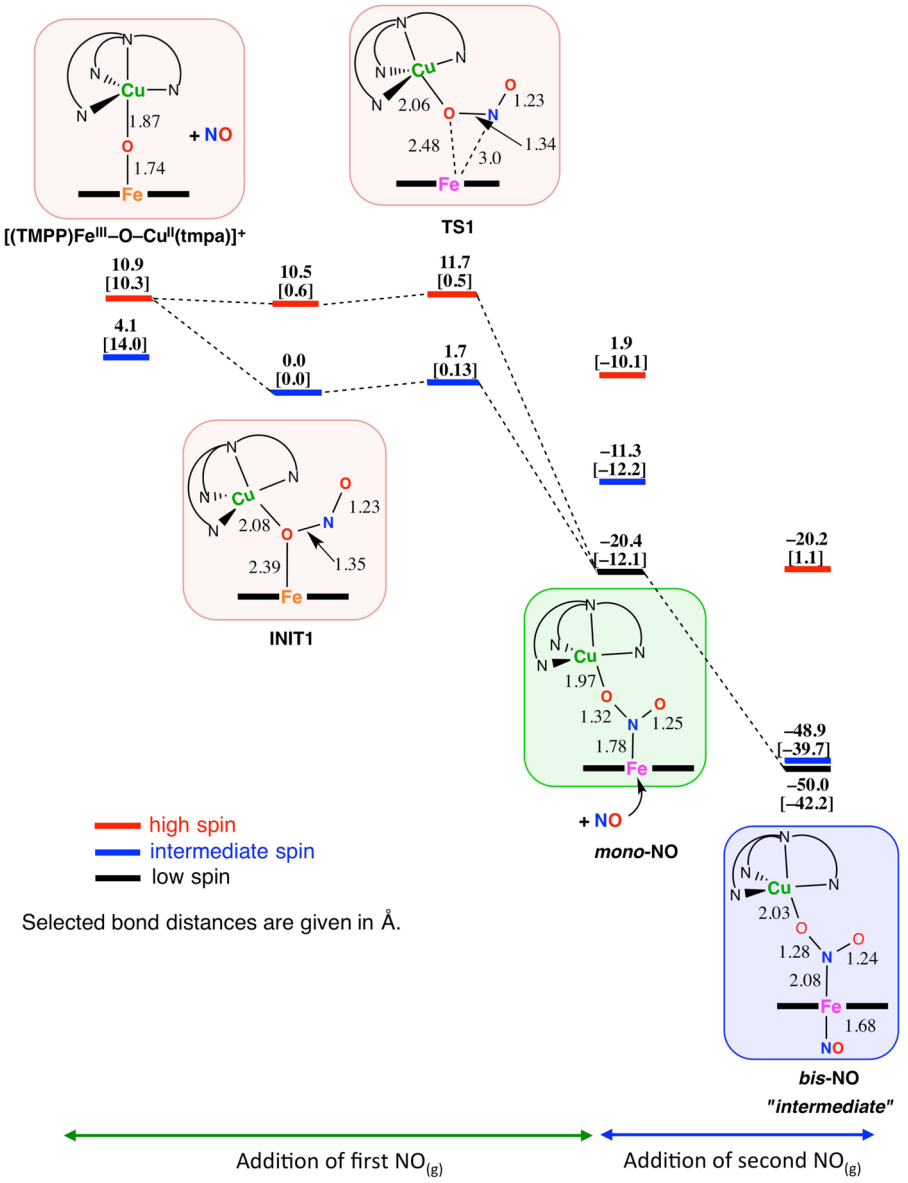

Adapted with permission from ref 11. Copyright 2015 American Chemical Society. [a]ΔE + ZPE in kcal mol^{-1} including solvent correction at both the BP86/6-31G(d) level and OLYP/6-311+G(d,p) level (given in brackets).

Scheme 7

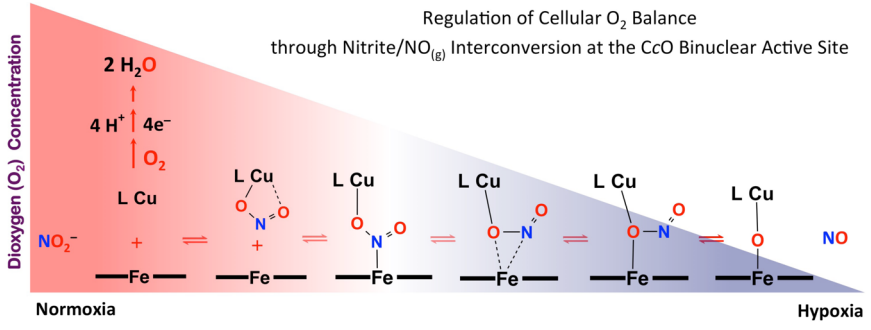

fragments, and availability and pK_a of proton sources, study of these factors is critical in order to fully understand C*c*O fuel-cell chemistry, that is, the O–O cleavage process, that pervades all of (bio)chemistry. Here, we briefly summarized past and very recent findings, which have led to the novel chemistry presented, a new powerful synthetic approach to generate many kinds of (new) heme/Cu constructs, which will allow for the future approaches and studies mentioned here. We have succeeded in

DOI: 10.1021/acs.accounts.5b00265
Acc. Chem. Res. 2015, 48, 2462–2474

the synthesis of heme−O_2−Cu complexes possessing distinctively varying properties of ligation, structure, spectroscopic features, and bonding. We are poised to examine the intimate details of stoichiometric reductive O−O cleavage reactions as a function of those heme−peroxo−Cu complex properties versus reducing agent power and proton source pK_a.

As we have also shown here, the same or similar heme/Cu constructs are able to readily effect one-electron nitrite reduction or $NO_{(g)}$ oxidation, occurring through *O*-atom transfer redox reactions. Molecular level structural and mechanistic details of these biologically relevant processes have been determined. The chemistry involved in these two processes is closely related; detailed kinetic−thermodynamic and spectroscopic studies reveal that they both proceed by essentially the same (but in opposite direction) pathways and require the involvement of common intermediates (Scheme 7). Of course, in C*c*O, these reactions also involve protons; in our synthetic models, these are not needed because the metal ions instead capture *O*-atoms or ions. Nevertheless, the studies here for the first time point to how these nitrogen oxide reactions can or do occur at heme/Cu centers and their relationship to dioxygen chemistry. These provide a basis for understanding the self-regulatory role of C*c*O in effecting cellular O_2 balance and its correlation to $NO_{(g)}$ and nitrite redox interplay with respect to hypoxia. Aside from further inquiries into heme/Cu/NO_x chemical systems, near-future goals include the interrogation of heme/Cu constructs for $NO_{(g)}$ reductive coupling, relevant to bacterial denitrification and $NO_{(g)}$ homeostasis.

AUTHOR INFORMATION

Corresponding Author

*E-mail: karlin@jhu.edu.

Author Contributions

The manuscript was written through contributions of all authors. All authors have given approval to the final version of the manuscript.

Notes

The authors declare no competing financial interest.

[§]Department of Chemistry, Southern Methodist University, Dallas, Texas 75275, United States.

Biographies

Shabnam Hematian, a native of Tehran, Iran, received her B.S. degree in chemistry from National University of Iran and M.S. degree in inorganic chemistry from Sharif University of Technology. In 2010, she joined the research group of Kenneth D. Karlin at Johns Hopkins University to work on heme/Cu/nitrogen oxides chemistry. She is currently a postdoctoral fellow at California Institute of Technology with Jonas C. Peters. Her research interests include metal-mediated small molecule activation.

Isaac Garcia-Bosch received his Ph.D. in Chemistry from the University of Girona in 2011 under the mentorship of Miquel Costas and Xavi Ribas. After his postdoctoral studies with Kenneth D. Karlin (Johns Hopkins University) as supported by a Marie Curie IOF Fellowship, he was appointed as Assistant Professor in the Department of Chemistry at Southern Methodist University in 2015. His research is focused on the development of first row metal complexes for O_2 reduction, H_2O oxidation, and bioinspired synthetic catalysis.

Kenneth D. Karlin is Ira Remsen Professor of Chemistry at Johns Hopkins University. His copper−dioxygen chemistry interests and research program were developed while at the State University of New York at Albany (1977−1989). He received his Ph.D. degree with Stephen J. Lippard from Columbia University (1975), and he was a NATO postdoctoral Fellow at the University of Cambridge (1975−1977). His research spans biologically inspired coordination chemistry of copper and heme/Cu systems with dioxygen and nitrogen oxides.

ACKNOWLEDGMENTS

The authors acknowledge financial support from the U.S.A. National Institutes of Health.

REFERENCES

(1) Yoshikawa, S.; Shinzawa-Itoh, K.; Nakashima, R.; Yaono, R.; Yamashita, E.; Inoue, N.; Yao, M.; Jei-Fei, M.; Libeu, C. P.; Mizushima, T.; Yamaguchi, H.; Tomizaki, T.; Tsukihara, T. Redox-Coupled Crystal Structure Changes in Bovine Heart Cytochrome *c* Oxidase. *Science* **1998**, *280*, 1723−1729.

(2) Kim, E.; Chufán, E. E.; Kamaraj, K.; Karlin, K. D. Synthetic Models for Heme-Copper Oxidases. *Chem. Rev.* **2004**, *104*, 1077−1133.

(3) Yoshikawa, S.; Shimada, A. Reaction Mechanism of Cytochrome c Oxidase. *Chem. Rev.* **2015**, *115*, 1936−1989.

(4) Solomon, E. I.; Heppner, D. E.; Johnston, E. M.; Ginsbach, J. W.; Cirera, J.; Qayyum, M.; Kieber-Emmons, M. T.; Kjaergaard, C. H.; Hadt, R. G.; Tian, L. Copper Active Sites in Biology. *Chem. Rev.* **2014**, *114*, 3659−3853.

(5) Castello, P. R.; David, P. S.; McClure, T.; Crook, Z.; Poyton, R. O. Mitochondrial Cytochrome Oxidase Produces Nitric Oxide under Hypoxic Conditions: Implications for Oxygen Sensing and Hypoxic Signaling in Eukaryotes. *Cell Metab.* **2006**, *3*, 277−287.

(6) Poyton, R. O.; Castello, P. R.; Ball, K. A.; Woo, D. K.; Pan, N. Mitochondria and Hypoxic Signaling. A New View. *Ann. N. Y. Acad. Sci.* **2009**, *1177*, 48−56.

(7) Nicholls, P.; Sharpe, M.; Torres, J.; Wilson, M. T.; Cooper, C. E. Nitric Oxide as an Effector and a Substrate for Cytochrome *c* Oxidase. *Biochem. Soc. Trans.* **1998**, *26*, S323.

(8) Torres, J.; Sharpe, M. A.; Rosquist, A.; Cooper, C. E.; Wilson, M. T. Cytochrome *c* Oxidase Rapidly Metabolises Nitric Oxide to Nitrite. *FEBS Lett.* **2000**, *475*, 263−266.

(9) Nanthakumar, A.; Fox, S.; Murthy, N. N.; Karlin, K. D.; Ravi, N.; Huynh, B. H.; Orosz, R. D.; Day, E. P.; Hagen, K. S.; Blackburn, N. J. Oxo- and Hydroxo-Bridged (Porphyrin)iron(III)-Copper(II) Species as Cytochrome *c* Oxidase Models: Acid-Base Interconversions and X-ray Structure of the Fe(III)-(O^{2-})-Cu(II) Complex. *J. Am. Chem. Soc.* **1993**, *115*, 8513−8514.

(10) Karlin, K. D.; Nanthakumar, A.; Fox, S.; Murthy, N. N.; Ravi, N.; Huynh, B. H.; Orosz, R. D.; Day, E. P. X-ray Structure and Physical Properties of the Oxo-Bridged Complex [(F_8-TPP)Fe-O-Cu-(TMPA)]$^+$, F_8-TPP = Tetrakis(2,6-difluorophenyl)porphyrinate(2-), TMPA = Tris(2-pyridylmethyl)amine: Modeling the Cyhtochrome *c* Oxidase Fe-Cu Heterodinuclear Active Site. *J. Am. Chem. Soc.* **1994**, *116*, 4753−4763.

(11) Hematian, S.; Kenkel, I.; Shubina, T. E.; Dürr, M.; Liu, J. J.; Siegler, M. A.; Ivanovic-Burmazovic, I.; Karlin, K. D. Nitrogen Oxide Atom-Transfer Redox Chemistry; Mechanism of $NO_{(g)}$ to Nitrite Conversion Utilizing μ-oxo Heme-Fe^{III}−O−Cu^{II}(L) Constructs. *J. Am. Chem. Soc.* **2015**, *137*, 6602−6615.

(12) Fox, S.; Nanthakumar, A.; Wikström, M.; Karlin, K. D.; Blackburn, N. J. XAS Structural Comparisons and Reversibly Interconvertible Oxo- and Hydroxo-Bridged Heme-Copper Oxidase Model Compounds. *J. Am. Chem. Soc.* **1996**, *118*, 24−34.

(13) Kopf, M.-A.; Neuhold, Y.-M.; Zuberbühler, A. D.; Karlin, K. D. Oxo- and Hydroxo-Bridged Heme-Copper Assemblies Formed from Acid-Base or Metal-Dioxygen Chemistry. *Inorg. Chem.* **1999**, *38*, 3093−3102.

(14) Ghiladi, R. A.; Hatwell, K. R.; Karlin, K. D.; Huang, H.-w.; Moënne-Loccoz, P.; Krebs, C.; Huynh, B. H.; Marzilli, L. A.; Cotter, R. J.; Kaderli, S.; Zuberbühler, A. D. Dioxygen Reactivity of Mononuclear

DOI: 10.1021/acs.accounts.5b00265
Acc. Chem. Res. 2015, 48, 2462−2474

Heme and Copper Components Yielding A High-Spin Heme-Peroxo-Cu Complex. *J. Am. Chem. Soc.* **2001**, *123*, 6183−6184.
(15) Chufán, E. E.; Puiu, S. C.; Karlin, K. D. Heme-Copper/Dioxygen Adduct Formation, Properties, and Reactivity. *Acc. Chem. Res.* **2007**, *40*, 563−572.
(16) Chishiro, T.; Shimazaki, Y.; Tani, F.; Tachi, Y.; Naruta, Y.; Karasawa, S.; Hayami, S.; Maeda, Y. Isolation and Crystal Structure of a Peroxo-Bridged Heme-Copper Complex. *Angew. Chem., Int. Ed.* **2003**, *42*, 2788−2791.
(17) Kim, E.; Shearer, J.; Lu, S.; Moënne-Loccoz, P.; Helton, M. E.; Kaderli, S.; Zuberbühler, A. D.; Karlin, K. D. Heme/Cu/O_2 Reactivity: Change in Fe^{III}-(O_2^{2-})-Cu^{II} Unit Peroxo Binding Geometry Effected by Tridentate Copper Chelation. *J. Am. Chem. Soc.* **2004**, *126*, 12716−12717.
(18) Chufan, E. E.; Mondal, B.; Gandhi, T.; Kim, E.; Rubie, N. D.; Moenne-Loccoz, P.; Karlin, K. D. Reactivity Studies on Fe^{III}-(O_2^{2-})-Cu^{II} Compounds: Influence of the Ligand Architecture and Copper Ligand Denticity. *Inorg. Chem.* **2007**, *46*, 6382−6394.
(19) Kieber-Emmons, M. T.; Qayyum, M. F.; Li, Y.; Halime, Z.; Hodgson, K. O.; Hedman, B.; Karlin, K. D.; Solomon, E. I. Spectroscopic Elucidation of a New Heme/Copper Dioxygen Structure Type: Implications for O···O Bond Rupture in Cytochrome c Oxidase. *Angew. Chem., Int. Ed.* **2012**, *51*, 168−172.
(20) Garcia-Bosch, I.; Adam, S. M.; Schaefer, A. W.; Sharma, S. K.; Peterson, R. L.; Solomon, E. I.; Karlin, K. D. A "Naked" Fe^{III}-(O_2^{2-})-Cu^{II} Species Allows for Structural and Spectroscopic Tuning of Low-Spin Heme-Peroxo-Cu Complexes. *J. Am. Chem. Soc.* **2015**, *137*, 1032−1035.
(21) Halime, Z.; Kieber-Emmons, M. T.; Qayyum, M. F.; Mondal, B.; Gandhi, T.; Puiu, S. C.; Chufán, E. E.; Sarjeant, A. A. N.; Hodgson, K. O.; Hedman, B.; Solomon, E. I.; Karlin, K. D. Heme-Copper-Dioxygen Complexes: Toward Understanding Ligand-Environmental Effects on the Coordination Geometry, Electronic Structure, and Reactivity. *Inorg. Chem.* **2010**, *49*, 3629−3645.
(22) Blomberg, M. R. A.; Siegbahn, P. E. M.; Wikström, M. A metal-bridging mechanism for O-O bond cleavage in cytochrome c oxidase. *Inorg. Chem.* **2003**, *42*, 5231−5243.
(23) Fee, J. A.; Case, D. A.; Noodleman, L. Toward a Chemical Mechanism of Proton Pumping by the B-Type Cytochrome c Oxidases: Application of Density Functional Theory to Cytochrome ba_3 of Thermus thermophilus. *J. Am. Chem. Soc.* **2008**, *130*, 15002−15021.
(24) If one starts with a heme-Fe^{III}−superoxide Cu(I) species (a model for compound **A**, Figure 1), at least two electrons are still required (e.g., from Cu(I), the active site tyrosine, or iron) to cleave the O−O bond. Our peroxo complexes are at the stage of having one more electron (from Cu(I)); we are thus poised to study the O−O cleavage step. The ultimate goal is to determine what factors pertaining to (heme)Fe−O_2−Cu ligation, structure and bonding, and electron reducing ability ($E°$) or proton acidity (pK_a) allow for (or not) O−O reductive cleavage without leakage of H_2O_2 or hydroxyl radical.
(25) Lehnert, N.; Berto, T. C.; Galinato, M. G. I.; Goodrich, L. E. The Role of Heme-Nitrosyls in the Biosynthesis, Transport, Sensing, and Detoxification of Nitric Oxide (NO) in Biological Systems: Enzymes and Model Complexes. In *The Handbook of Porphyrin Science*; Kadish, K. M.; Smith, K.; Guilard, R., Eds.; World Scientific: Singapore, 2011; Vol. *14*, pp 1−247.
(26) Shiva, S.; Wang, X.; Ringwood, L. A.; Xu, X.; Yuditskaya, S.; Annavajjhala, V.; Miyajima, H.; Hogg, N.; Harris, Z. L.; Gladwin, M. T. Ceruloplasmin is a NO oxidase and nitrite synthase that determines endocrine NO homeostasis. *Nat. Chem. Biol.* **2006**, *2*, 486−493.
(27) Hematian, S.; Siegler, M. A.; Karlin, K. D. Heme/Copper Assembly Mediated Nitrite and Nitric Oxide Interconversion. *J. Am. Chem. Soc.* **2012**, *134*, 18912−18915.
(28) Hematian, S.; Siegler, M. A.; Karlin, K. D. Nitric Oxide Generation from Heme/Copper Assembly Mediated Nitrite Reductase Activity. *JBIC, J. Biol. Inorg. Chem.* **2014**, *19*, 515−528.
(29) Merkle, A. C.; Lehnert, N. Binding and activation of nitrite and nitric oxide by copper nitrite reductase and corresponding model complexes. *Dalton Trans.* **2012**, *41*, 3355−3368.
(30) Maia, L. B.; Moura, J. J. G. How Biology Handles Nitrite. *Chem. Rev.* **2014**, *114*, 5273−5357.
(31) Yi, J.; Heinecke, J.; Tan, H.; Ford, P. C.; Richter-Addo, G. B. The Distal Pocket Histidine Residue in Horse Heart Myoglobin Directs the O-Binding Mode of Nitrite to the Heme Iron. *J. Am. Chem. Soc.* **2009**, *131*, 18119−18128.
(32) Loullis, A.; Noor, M. R.; Soulimane, T.; Pinakoulaki, E. The Structure of a Ferrous Heme-Nitro Species in the Binuclear Heme a_3/Cu_B Center of ba_3-Cytochrome *c* Oxidase as Determined by Resonance Raman Spectroscopy. *Chem. Commun.* **2015**, *51*, 286−289.
(33) Collaboration with the University of Erlangen-Nuremberg group. See ref 11.
(34) In the C*c*O active site, the heme possesses an axial proximal histidine ligand, which can be considered to be taking the place of the second $NO_{(g)}$ molecule in our synthetic system.

DOI: 10.1021/acs.accounts.5b00265
Acc. Chem. Res. 2015, 48, 2462−2474